Cholesterol-Rich Plasma Membrane Domains (Lipid Rafts) in Keratinocytes: Importance in the Baseline and UVA-Induced Generation of Reactive Oxygen Species

Robert Gniadecki, Nanna Christoffersen, and Hans Christian Wulf

Department of Dermatology, University of Copenhagen, Bispebjerg Hospital, Copenhagen, Denmark

The biologic effects of ultraviolet radiation such as DNA damage, mutagenesis, cellular aging, and carcinogenesis are in part mediated by reactive oxygen species. In unirradiated cells the major known sources of reactive oxygen species are the mitochondrial respiratory chain and the membrane oxidases functionally coupled to several membrane growth factor receptors. There is evidence that mitochondria also play a role in oxidative stress after ultraviolet irradiation; however, it is unknown whether the biochemical processes at the level of the plasma membrane contribute to the regulation of reactive oxygen species synthesis. In order to elucidate this issue we examined here the importance of the microdomain plasma membrane organization in the regulation of oxidative stress in unirradiated and ultraviolet A (340–400 nm) irradiated HaCaT keratinocytes. Labeling of confluent HaCaT cultures with fluorescently tagged cholera toxin B subunit (FITC-CTx) revealed the presence of GM1 ganglioside and cholesterol-rich microdomains (lipid rafts) that formed junction-like structures in the membranes of adjacent cells and patchy microdomains elsewhere. There was a marked heterogeneity in the level of FITC-CTx labeling: there were groups of cells demonstrating prominent labeling (FITC-CTx^{high}) whereas other cells were only weakly labeled (FITC-CTx^{low}). When reactive oxygen species synthesis was measured with the fluorescent probe carboxy-2′,7′-dichlorodihydrofluorescein diacetate, we found that (i) the baseline and ultraviolet-A-induced reactive oxygen species synthesis correlated with the magnitude of FITC-CTx labeling and was highest in the FITC-CTx^{high} cells; (ii) reactive oxygen species synthesis was diminished in cells in which the integrity of membrane domains was disrupted by cholesterol sequestration with methyl-β-cyclodextrin and filipin, or after treatment with GM1 ganglioside; (iii) reactive oxygen species synthesis in cholesterol-depleted cells was fully restored after cholesterol repletion. We conclude that the plasma membrane takes part in the regulation of oxidative stress in keratinocytes and disruption of its microdomain structure reduces reactive oxygen species synthesis both at the baseline and after ultraviolet A irradiation. We hypothesize that lipid-raft-associated protein(s) may be involved in the generation of reactive oxygen species and that pharmacologic modulation of membrane structure may provide a novel therapeutic approach relevant for photoprotection and cutaneous carcinogenesis.

Key words: free radicals/gangliosides/membrane lipids/ultraviolet radiation. J Invest Dermatol 118:582–588, 2002

Irradiation of cells with ultraviolet (UV) radiation induces the production of reactive oxygen species (ROS). In many tissues, including the skin, ROS have been implicated as mediators of apoptosis, cellular aging, and carcinogenesis (Chen and Ames, 1994; Lu *et al*, 1997; Morita *et al*, 1997). The central question is the molecular mechanism by which ROS are synthesized in the cells. In unirradiated cells there is a steady-state ROS synthesis, mostly due to an imperfect, one electron reduction of oxygen to superoxide in the respiratory chain in mitochondria (Chance *et al*, 1979; Nohl and Jordan, 1986; Hansford *et al*, 1997). This process is augmented in mitochondria that have lost their transmembrane potential $\Delta\Psi_m$, e.g., during early stages of apoptosis (Zamzami *et al*, 1995; Quillet-Mary *et al*, 1997). Some recent data indicate that events at the level of the plasma membrane are also involved in ROS metabolism. Activation of some tyrosine kinase receptors may result in induction of ROS as second messenger. For example, hydrogen peroxide is generated in response to the activation of epidermal growth factor (EGF) receptor and platelet-derived growth factor (PDGF) receptor and is dependent upon activation of phosphatidylinositol 3-kinase and the small G-protein Rac (Irani *et al*, 1997; Bae *et al*, 1999, 2000).

The mechanism of ROS induction in response to UV irradiation is less well understood. In contrast to early concepts regarding the UV-dependent ROS synthesis as a passive photochemical reaction, recent studies indicate that it is an actively regulated metabolic process involving cytoplasmic and mitochondrial oxidases (Hockberger *et al*, 1999; Zorov *et al*, 2000; Gniadecki *et al*,

Manuscript received June 8, 2001; revised October 23, 2001; accepted for publication November 30, 2001.

Reprint requests to: Dr. Robert Gniadecki, D.M.Sci., Department of Dermatology D92, Bispebjerg Hospital, Bispebjerg bakke 23, DK-2400 Copenhagen NV, Denmark. Email: rgniadecki@hotmail.com

Abbreviations: carboxy-DCF, carboxy-2′,7′-dichlorofluorescein; carboxy-H_2DCFDA, carboxy-2′,7′-dichlorodihydrofluorescein diacetate; FITC-CTx, fluorescently tagged cholera toxin B subunit.

2001). In this study we asked whether the biochemical events at the plasma membrane level are of importance by studying the significance of cholesterol-rich membrane rafts for ROS synthesis in cultured keratinocytes. The rationale for this approach is based on the fact that raft structures play a pivotal role in the regulation of membrane signal transduction in eucaryotic cells.

Lipid rafts are focal assemblies of cholesterol and sphingolipids in plasma membranes and demonstrate decreased fluidity in comparison to the lipids in the surrounding portions of the membrane (Simons and Ikonen, 1997). The lipids composing raft microdomains are selectively enriched in sphingolipids with saturated hydrocarbon chains that associate tightly with cholesterol to produce a higher-order lipid structure than that achieved by the nonraft unsaturated phospholipid–cholesterol aggregates (Sankaram and Thompson, 1990). The presence of lipid rafts has been shown in different cell types including lymphocytes (Janes *et al*, 1999), basophils (Wilson *et al*, 2000), and various fibroblastoid and leukemia cell lines (Stauffer and Meyer, 1997; Harder *et al*, 1998).

The main physiologic importance of lipid rafts is their key role in the regulation of the chemical activity of cholesterol in the membranes (Radhakrishnan and McConnell, 2000) and the participation in the processes of signal transduction in eucaryotic cells (reviewed by Simons and Toomre, 2000). Cholesterol-rich raft microdomains can include or exclude membrane proteins, probably on the basis of the hydrophobic properties within the transmembrane domains (Scheiffele *et al*, 1997) or due to some post-translational modifications such as palmitoylation (Melkonian *et al*, 1999). Some crucial signaling proteins such as T cell receptor complex, FcεRI, G-proteins, Src-like tyrosine kinases, Hedgehog, EGF receptor, or Ras proteins have affinity to rafts (Simons and Toomre, 2000) and their association with rafts seems to be a prerequisite for signal transduction. Convincing evidence supporting the importance of rafts for signal transduction has been generated by showing that raft disruption in living cells *in vivo* inhibited cellular signaling pathways. For example, FcεRI, T cell receptor, or Ras signaling could be abolished when surface cholesterol was depleted with methyl-β-cyclodextrin but was restored after cholesterol replenishment (Moran and Miceli, 1998; Xavier *et al*, 1998; Roy *et al*, 1999). Moreover, activation of signal transduction by cross-linking membrane receptors with appropriate ligands is associated with aggregation of nanometer-sized rafts into microdomains several microns in size (Stauffer and Meyer, 1997; Janes *et al*, 1999).

One of the best established methods to visualize raft aggregates in cells *in situ* is tagging of ganglioside GM1 with fluorescently labeled cholera toxin B (FITC-CTx) (Fra *et al*, 1994; Harder *et al*, 1998; Janes *et al*, 1999). Ganglioside GM1 is exclusively found in rafts and may therefore be considered as a raft marker (Harder *et al*, 1998; Radhakrishnan *et al*, 2000). In the experiments described in this paper we employed the FITC-CTx staining method to follow the emergence of lipid raft aggregates in the cultured keratinocyte cell line HaCaT and examined the involvement of rafts in the processes of generation of ROS.

MATERIALS AND METHODS

Cell culture HaCaT keratinocyte cells (Boukamp *et al*, 1988) were seeded at 7×10^3 cells per cm^2 and cultured in Dulbecco's minimal essential medium (DMEM, Gibco, Rockville, MD) with 10% (vol/vol) heat-inactivated fetal bovine serum (Gibco) at 37°C in an atmosphere of 100% humidity and 5% CO_2. For the experiments we included the cells from 24 h cultures (nonconfluent, single attached cells) or from 1-wk-old cultures (95%–100% confluent). Cell viability was monitored using the Trypan Blue exclusion assay and in each experiment exceeded 95%.

UVA irradiation The UVA source consisted of an array of three Philips TL 10R tubes (Philips, Eindhoven, The Netherlands) that emits UVA1 radiation (341–400 nm, peak 367 nm) at an intensity of 3.7 mW per cm^2. The emitted intensities were measured using an International Light 1700 research radiometer with a SED 400 detector as described previously (Gniadecki *et al*, 2001). Before irradiation the media were changed into phosphate-buffered saline (PBS) and the cells were irradiated from above. To prevent overheating of the media during irradiation the culture vessels rested on a 5 mm thick plastic plate placed on an ice-water slurry. The control cells were handled as the experimental cells but were shielded from UVA with a piece of aluminum foil.

Determination of ROS synthesis Intracellular levels of ROS were measured with a semiquantitative assay using carboxy-2′,7′-dichlorodihydrofluorescein diacetate (carboxy-H_2DCFDA, Molecular Probes, Eugene, OR), essentially as described in the previous work from this laboratory (Gniadecki *et al*, 2001). After entering the cell the esterases hydrolyze the compound into a nonfluorescent intermediate carboxy-2′,7′-dichlorodihydrofluorescein, which is retained inside the cell due to the large negative charge of the molecule. Oxidation by ROS causes a further conversion into fluorescent carboxy-2′,7′-dichlorofluorescein (carboxy-DCF). The cells were loaded with 10 μM carboxy-H_2DCFDA in PBS for 30 min at 37°C. Cells were fixed in 2% ice-cold buffered paraformaldehyde for 10 min. The carboxy-DCF fluorescence was measured with laser scanning cytometry or confocal microscopy, as described below. For control experiments we replaced carboxy-H_2DCFDA with an oxidized fluorescent probe carboxy-2′,7′-dichlorofluorescein diacetate (Molecular Probes) to eliminate the possibility that any observed differences in fluorescence are caused by alterations in esterase activity or efflux of the probe from the cells. Moreover, to eliminate the possibility that observed changes in carboxy-DCF fluorescence are caused by a direct photochemical reaction initiated by UVA, the solutions of carboxy-H_2DCFDA and carboxy-2′,7′-dichlorodihydrofluorescein intermediate (Molecular Probes) were prepared in PBS and 20 μl of each solution was loaded into a 10 mm × 7 mm (width × length) chamber created between the coverslip attached to the microscope slide by double adhesive 3M tape. The same chamber was used for laser scanning cytometry of the cells (see below and Clatch *et al*, 1998; Gniadecki *et al*, 2001). The chambers were irradiated from above with different doses of UVA1 in the same conditions as used in the case of the cells. In a preliminary experiment it was determined that the attenuation of UVA1 radiation intensity by the coverslip was negligible. The carboxy-DCF fluorescence was determined by confocal laser scanning microscopy, as detailed below.

Cholesterol depletion and repletion A stock solution of 10% methyl-β-cyclodextrin (Sigma, St. Loius, MO) was prepared in PBS. Cholesterol/methyl-β-cyclodextrin stock was obtained by dissolving 20 mg per ml water-soluble cholesterol (Sigma) in PBS and further diluting × 50 in 10% methyl-β-cyclodextrin. Cells were washed twice with PBS and cholesterol was depleted and repleted using the slightly modified procedure described by Furuchi and Anderson (1998) and Roy *et al* (1999). Briefly, the media were changed to DMEM and the cells were incubated with different concentrations of methyl-β-cyclodextrin for 30 min at 37°C and washed twice in PBS. Cholesterol repletion was achieved by incubation with final 80 μg per ml cholesterol and 0.2% methyl-β-cyclodextrin for 30 min at 37°C.

Incubation with filipin and GM1 ganglioside Stock solutions of filipin (Sigma) and purified bovine brain GM1 ganglioside (supplied by Professor Barbara Gajkowska, Laboratory of Cell Ultrastructure, Polish Academy of Sciences, Warsaw, Poland) were prepared in PBS. The cells were incubated with final 10 μg per ml filipin or 50 μM GM1 ganglioside in PBS for 30 min at 37°C.

FITC-CTx staining The cells were fixed with 2% ice-cold buffered paraformaldehyde for 10 min at 4°C followed by cell permeabilization in methanol at −20°C for 5 min (Osborn *et al*, 1988), or left unfixed, as indicated. The intensity of subsequent staining deteriorated slightly after the paraformaldehyde/methanol technique. FITC-CTx (Sigma) was dissolved in PBS with 5% bovine serum albumin (8 μg protein per ml) and the cells were incubated at 37°C for 30 min with occasional gentle rocking, essentially as described by Harder *et al* (1998). Before fluorescence microscopy the cells were washed twice with PBS. The images were obtained with an epifluorescence or confocal laser scanning inverted microscope, as described below.

Laser scanning cytometry The principle of laser scanning cytometry is similar to that of flow cytometry and its use for the measurements of carboxy-DCF fluorescence has been extensively described before (Gniadecki *et al*, 2001, and references therein). Briefly, suspension of HaCaT cells was coverslipped in the chamber slides (Clatch *et al*, 1998) and the cells were scanned in a laser scanning cytometry scanner (CompuCyte, Campridge, MA) using the 488 nm argon laser line as an excitation source. Fluorescence was gathered through a green 530 ± 30 nm filter. The objects corresponding to single cells were contoured using forward scatter, and integral green fluorescence (the sum

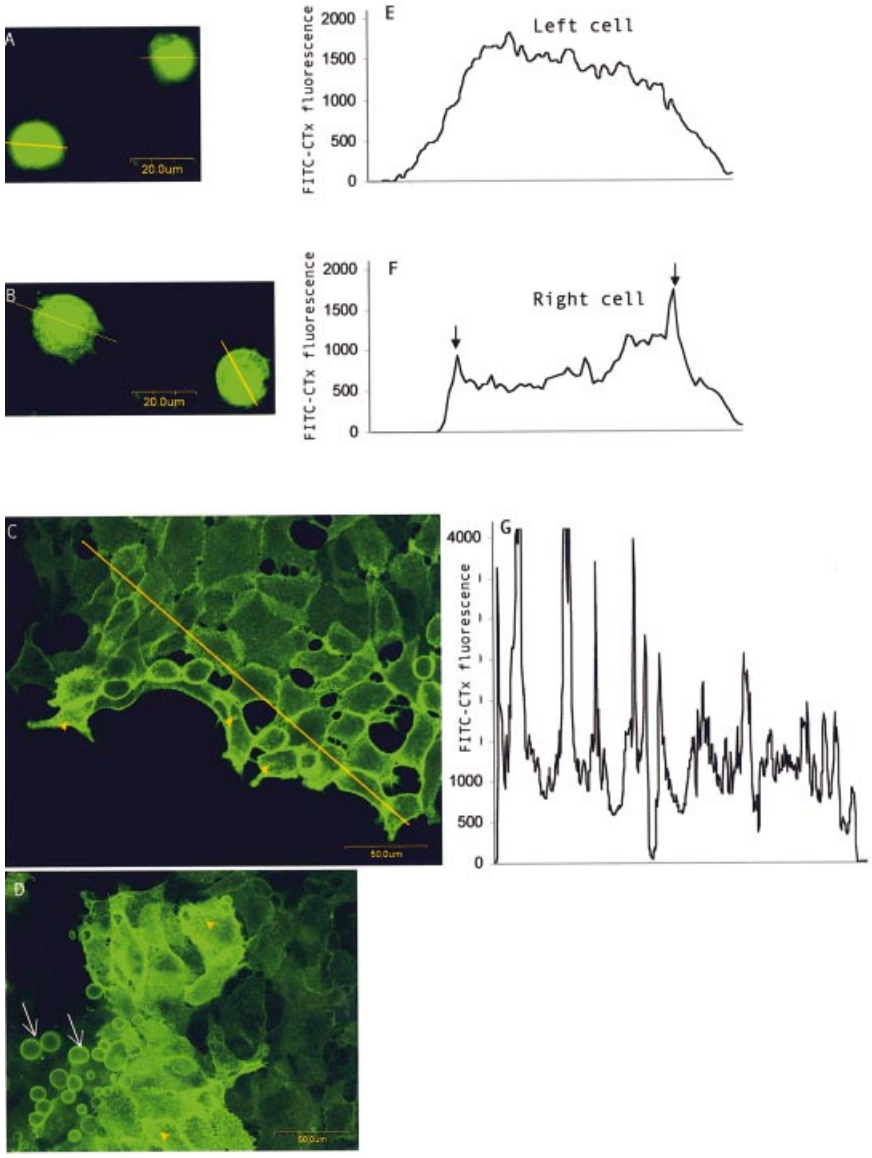

Figure 1. Plasma membrane microdomains (lipid rafts) in cultured HaCaT cells. (*A*)–(*D*) Confocal microscopy of unfixed, FITC-CTx-labeled cells: (*A*) trypsinized cells in suspension; (*B*) cells attached to glass; (*C*), (*D*) confluent cell cultures. *Yellow arrowheads* in (*C*), (*D*) show speckled GM1-ganglioside-enriched membrane domains stained with FITC-CTx; *white arrows* in (*D*) show GM1-ganglioside-enriched membrane vesicles. (*E*)–(*G*) Fluorescence intensity profiles along the scanning lines marked with yellow in (*A*)–(*C*). Enrichment of the peripheral part of the membrane in GM1 ganglioside is marked with *arrows* in (*F*). Note the presence of FITC-CTx^{high} and FITC-CTx^{low} cells in (*C*) and (*D*) and the formation of junctional lipid structures between adjacent cells (*C*, *D*, *G*).

of values of all pixels within the contour) was measured and shown as histograms using the proprietary Wincyte software. The scale of the *y* axis of the histograms was equalized to the highest peak of the curve to remove the differences due to the different amounts of cells analyzed in different experiments. Usually, 7000–10,000 cells were scanned in a single experiment.

Fluorescence microscopy An Olympus IX70 inverted microscope was used. The cells were grown on glass coverslips, stained, and observed directly, or trypsinized, coverslipped, and observed in suspension. For epifluorescence microscopy the xenon lamp was employed as an excitation source. For confocal microscopy, an Olympus Fluoview scanning unit equipped with an argon–krypton laser at 488 nm was used. During scanning of carboxy-H_2DCFDA-loaded cells we observed that prolonged (more than 5 s) irradiation with the xenon lamp or slow scanning with the 488 nm laser line causes probe oxidation and an artifactual increase in fluorescence. To avoid this artifact the cells were initially brought in focus using standard epifluorescence. Then the epifluorescence was switched off and the specimen was moved beyond the previously illuminated area. A single scan at one focal plane was obtained and the image was saved for subsequent measuring of fluorescence intensity with the Olympus proprietary software. In the case of scanning of the control and irradiated solutions of carboxy-H_2DCFDA and carboxy-2′,7′-dichlorodihydrofluorescein the microscope was focused in the middle of the coverslipped fluid slab and the 20× objective with larger than optimal pinhole was used in addition to the 40× objective in order to obtain the larger confocal layer thickness. The results obtained with the 20× objective did not differ from the results with the 100× objective.

RESULTS

Redistribution of ganglioside GM1, cholesterol-rich membrane microdomains in cultured HaCaT cells In the first series of experiments we investigated the presence of cholesterol-rich microdomains (lipid rafts and/or raft aggregates) in plasma membrane in cultured keratinocytes. These microdomains were visualized by fluorescence tagging with FITC-CTx, which selectively binds to ganglioside GM1, a marker of lipid rafts (Harder *et al*, 1998; Radhakrishnan *et al*, 2000). Unattached HaCaT cells in suspension demonstrated a homogeneous distribution of FITC-CTx fluorescence with no discernible domains (**Fig 1*A*, *E***). Twenty-four hours after plating a redistribution of GM1 ganglioside towards cell margins occurred (**Fig 1*B*, *F***) and the staining pattern and staining level were similar in all cells. The FITC-CTx staining pattern changed radically in the cells that reached confluence. Ganglioside GM1 redistributed to the membrane portions of adjacent HaCaT cells forming junction-like structures (**Fig 1*C*, *D*, *G***). Additionally, there was a speckled staining of the membranes with a spot size of several microns.

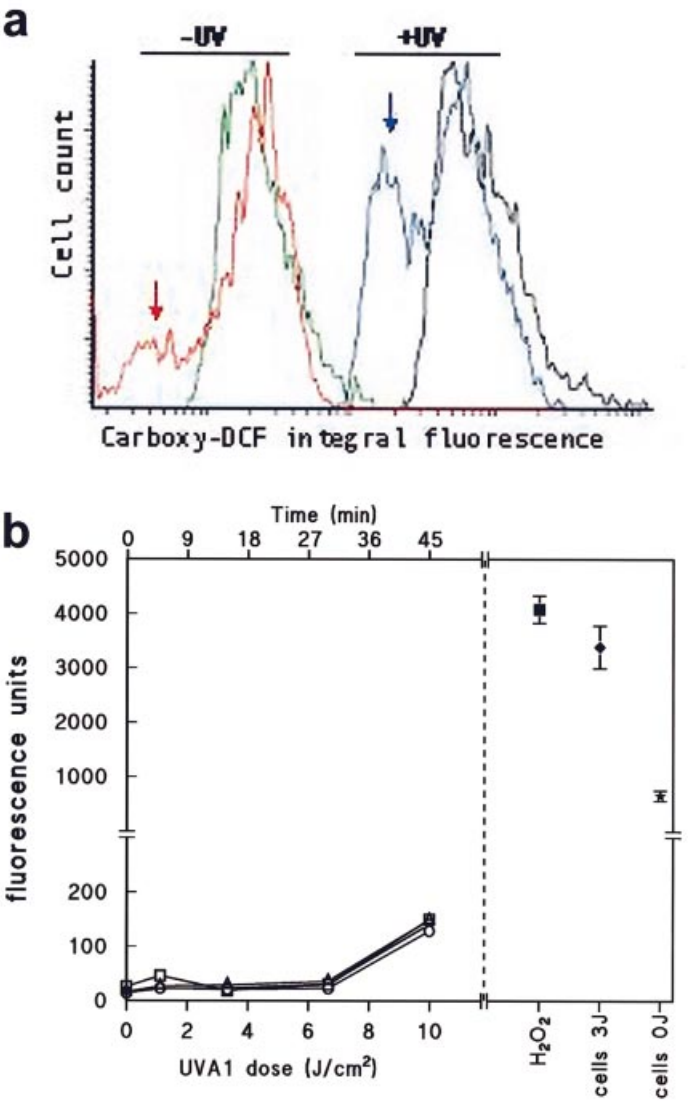

Figure 2. ROS formation in nonconfluent and confluent HaCaT cells. (*a*) The cells were cultured for 24 h (nonconfluent cells, green and black lines) or 1 wk (confluent cells, red and blue lines), loaded with carboxy-H_2DCFDA, and irradiated with 3 J per cm^2 UVA (blue, black) or sham-irradiated (green, red). The cells were released by trypsinization and fixed, and the integral carboxy-DCF fluorescence was measured by laser scanning cytometry. Note the presence of a subpopulation of cells showing lower fluorescence in confluent cultures (*arrows*), both before and after irradiation. (*b*) Control experiment showing the degree of oxidation of carboxy-H_2DCFDA and carboxy-2′,7′-dichlorodihydrofluorescein in PBS solution. Twenty microliters of 10 μM or 1 mM (not shown) of each solution was coverslipped and irradiated with the increasing doses of UVA1 indicated on the lower *x* axis (carboxy-H_2DCFDA, *open circles*; carboxy-2′,7′-dichlorodihydrofluorescein, *open squares*). The corresponding times of irradiation are shown on the upper *x* axis. Other samples were left in subdued ambient light conditions in which the whole experiment was performed (carboxy-H_2DCFDA, *open semicircles*; carboxy-2′,7′-dichlorodihydrofluorescein, *open triangles*) for the periods of time indicated on the upper *x* axis. As a positive control we used the carboxy-H_2DCFDA or carboxy-2′,7′-dichlorodihydrofluorescein solutions incubated for 15 min in 100 mM hydrogen peroxide (*closed square*). Additionally, the level of fluorescence obtained from unirradiated cells (cells 0J, star) and cells irradiated with 3 J per cm^2 (cells 3J, closed diamond) are plotted. The irradiated or control slides were scanned in a confocal laser scanning microscope and the fluorescence in the scanned area was measured using the proprietary Olympus FluoView software. Data show mean values from three independent experiments (each experiment was performed in duplicate); whiskers show SD. For clarity some means are shown without SD; in these instances the SD values were < 7% of the mean.

There was a marked heterogeneity in the level of staining: in the confluent sheath of keratinocytes one could discern islands comprising 5–30 cells with a very high degree of FITC-CTx staining (FITC-CTx^{high}) whereas the surrounding cells demonstrated a 10–100-fold reduced fluorescence (FITC-CTx^{low}). Sometimes, in confluent cells the FITC-CTx^{high} cells produced cytoplasmic blebbing with a high degree of FITC-CTx staining (**Fig 1*G***).

Cholesterol depletion with methyl-β-cyclodextrin and filipin or treatment with GM1 ganglioside reduce the baseline and UVA-stimulated ROS synthesis The confluent and nonconfluent cultures were stained with carboxy-H_2DCFDA to compare the level of unstimulated (endogenous) ROS synthesis. The 24-h-old cultures containing mostly nonconfluent attached single cells demonstrated a homogeneous population of cells with high carboxy-DCF fluorescence (**Fig 2**); heterogeneity was observed in confluent cultures. Often, as shown in **Fig 2**, two subpopulations of cells, one exhibiting a higher degree of baseline carboxy-DCF fluorescence of a level similar to the nonconfluent cells and one with an integrated fluorescence approximately a magnitude lower, were present. Sometimes, these two populations were overlapping and in these cases the carboxy-DCF histogram peak was broad, spanning at least two magnitudes of integrated fluorescence (see, for example, **Fig 4**).

A similar pattern was observed after irradiation with UVA. Nonconfluent, single cells showed a uniform increase in fluorescence, whereas two subpopulations or a broad integrated fluorescence peak was present in confluent cells (**Fig 2*a***).

To determine whether the difference in carboxy-DCF fluorescence between confluent and nonconfluent cells could be correlated with FITC-CTx labeling pattern, the cells were labeled with carboxy-H_2DCFDA, scanned in the confocal microscope, and restained with FITC-CTx after removal of fluorescent carboxy-DCF. **Figure 3** shows that high carboxy-DCF staining was chiefly present in FITC-CTx^{high} cells.

Methyl-β-cyclodextrin is a cyclic polysaccharide-containing hydrophobic cavity enabling extraction of cholesterol from membranes (Radhakrishnan and McConnell, 2000). Therefore, we investigated whether disruption of cholesterol-enriched domains with methyl-β-cyclodextrin may alter the baseline ROS synthesis. A short-term 30 min treatment with methyl-β-cyclodextrin did not change the FITC-CTx staining pattern and did not change the gross morphology of cultured cells (not shown) but dramatically reduced the level of carboxy-DCF fluorescence (**Fig 4*A***, ***B***). This finding was reinforced by data showing that cholesterol sequestration with 1 h treatment with filipin, a sterol-binding agent (Fagan *et al*, 2000), or treatment with ganglioside GM1 had an effect similar to that obtained with methyl-β-cyclodextrin (**Fig 4*B***).

The oxidation of carboxy-H_2DCFDA by UVA1 required a cellular context as the UVA1 irradiation of PBS solutions of carboxy-H_2DCFDA and the intercellular intermediate carboxy-2′,7′-dichlorodihydrofluorescein did not result in an appreciable increase in carboxy-DCF fluorescence at the doses used for cell irradiation. Fluorescence increase was seen after very prolonged irradiations or even incubations, however, probably due to the oxidative action of the dissolved oxygen (**Fig 2*b***). As this did not have any significance for this study we did not further investigate this phenomenon. Moreover, to exclude the possibility that the loss of carboxy-DCF fluorescence was due to an increased membrane permeability and probe leakage or/and altered esterase activity in methyl-β-cyclodextrin- and filipin-treated cells a control experiment was performed where the cells were loaded with carboxy-2′,7′-dichlorofluorescein diacetate and the fluorescence was measured after treatment with both raft-disrupting agents. A small decrease of fluorescence (range 5%–15%, three independent experiments) was noted in the filipin-treated cells but no change was evident in the methyl-β-cyclodextrin- or GM1-ganglioside-treated cells. In another control experiment the cellular depletion of

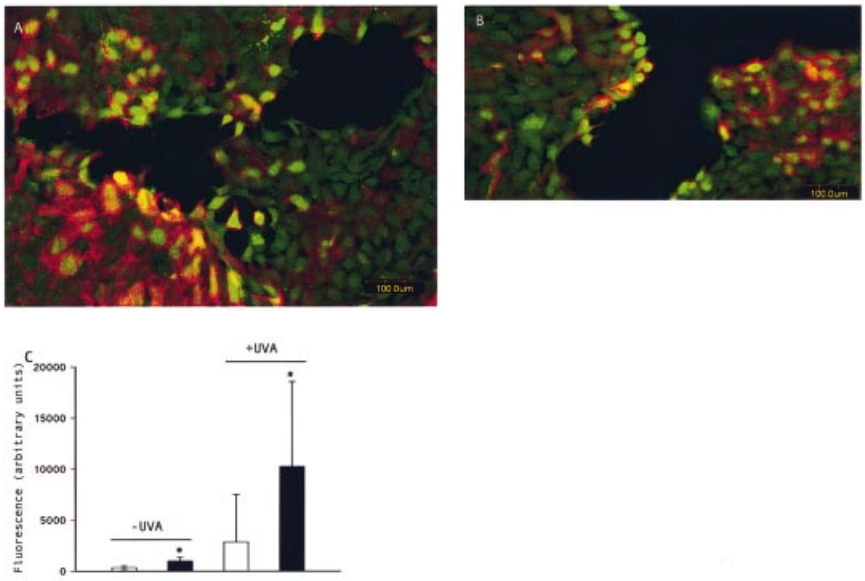

Figure 3. Relationship between FITC-CTx staining and ROS synthesis in confluent HaCaT cells. The cells were loaded with carboxy-H_2DCFDA and sham-irradiated (*A*) or irradiated with 3 J per cm^2 UVA (*B*). Then the carboxy-DCF fluorescence representing ROS synthesis was visualized with confocal microscopy (green color). Scanned cells were fixed with paraformaldehyde and permeabilized in methanol, which led to the complete loss of carboxy-DCF due to diffusion through the membranes. The cells were stained with FITC-CTx and re-scanned in the confocal microscope. GM1-ganglioside-rich domains are visualized with red color. The images were exported to Adobe Photoshop and overlayed using the "Multiple" mode in "Layers". (*C*) Quantitative assessment of carboxy-DCF fluorescence in FITC-CTx^{high} (solid) and FITC-CTx^{low} (open) cells. The cells were prepared as for (*A*), (*B*). Mean fluorescence ($n = 50$ cells) with SD/100 μm^2 cross-sectional surface of the cell are plotted. There was a statistically significant difference (*$p < 0.0001$, Mann–Whitney test) in carboxy-DCF fluorescence between FITC-CTx^{high} and FITC-CTx^{low} cells.

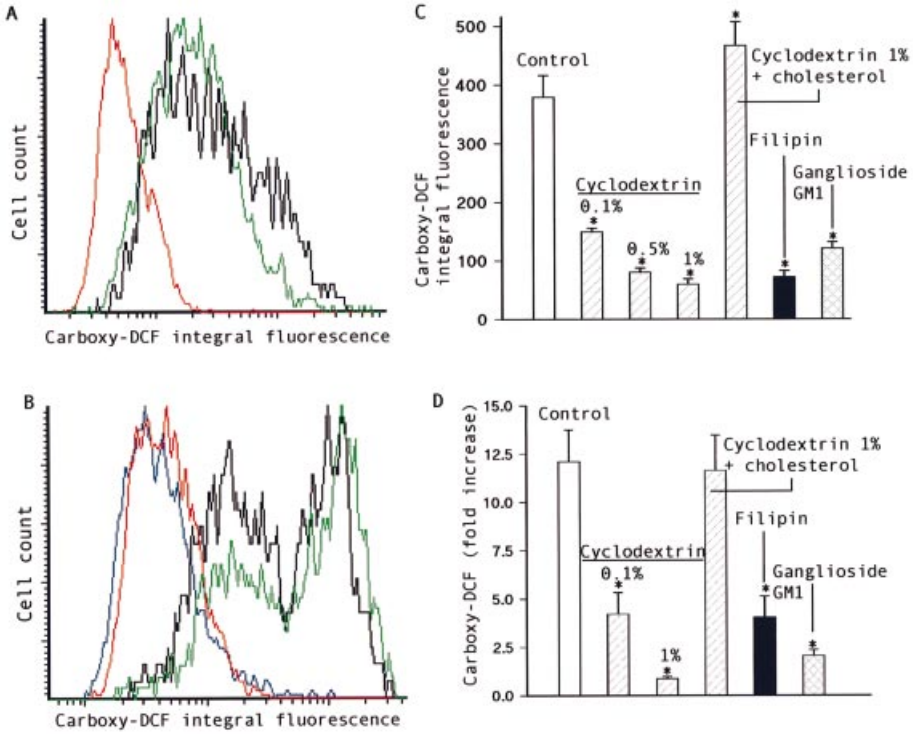

Figure 4. Effect of lipid raft integrity on intracellular ROS synthesis in HaCaT cells. Confluent cells were loaded with carboxy-H_2DCFDA and sham-irradiated (*A*, *B*) or irradiated with 3 J per cm^2 UVA (*C*, *D*). Before irradiation the structure of the rafts was disrupted with different concentrations of methyl-β-cyclodextrin, filipin, or GM1 ganglioside. Cells depleted of cholesterol with methyl-β-cyclodextrin were repleted by incubation with cyclodextrin/cholesterol. (*A*), (*B*) Representative histograms of carboxy-DCF fluorescence: green lines, control; red lines, effect of cholesterol depletion with 1% cyclodextrin; black lines, effect of cholesterol depletion and repletion with 1% cyclodextrin/cholesterol; blue line in (*C*), sham-irradiated cells. (*B*), (*C*) Mean (+ SD) carboxy-DCF fluorescence in all experimental groups. *$p < 0.001$ in comparison with the control, *t* test.

cholesterol was reversed by incubation with methyl-β-cyclodextrin/cholesterol complexes (**Fig 4*A*, *B***). These experiments showed that ROS-mediated oxidation of carboxy-H_2DCFDA was restored in cholesterol-repleted cells.

The above results led us to conclude that basal ROS synthesis in HaCaT cells depends on the integrity of cholesterol-rich domains in the plasma membrane. To investigate whether this is also true for ROS synthesis induced by UV the same line of experiments was executed in the carboxy-H_2DCFDA-loaded, UVA-irradiated cells. As shown in **Fig 3(*C*)** UVA-induced ROS synthesis was increased in FITC-CTx^{high} cells. ROS synthesis could be blocked by methyl-β-cyclodextrin, GM1 ganglioside, and filipin and was restored after cholesterol repletion in methyl-β-cyclodextrin-treated cells (**Fig 4*C*, *D***).

DISCUSSION

Results of this study show that cholesterol- and GM1-ganglioside-rich membrane domains (lipid rafts and raft aggregates) are present in the cultured keratinocyte cell line HaCaT and that they are rearranged during cell culturing. FITC-CTx staining showed that nonadherent cells in suspension do not demonstrate any discernible membrane domains. Upon attachment and cell spreading a peripheral staining of the membrane was seen whereas in confluent cells a strong patched and junctional labeling of the plasma membrane was noticed.

Formation of cholesterol-enriched raft-like domains between adjacent adherent cells has not been explicitly reported previously. In the paper of Mañes *et al* (1999), however, who examined the

importance of lipid rafts for cell mobility, one can notice an enhanced FITC-CTx staining in the contact regions between two adjacent breast MCF-7 adenocarcinoma cells. It is therefore likely that membranes of adherent cells are enriched in raft structures that probably form a platform for membrane proteins involved in cell–cell communication.

Cholesterol-rich blebs were sometimes observed in the raft-enriched regions, which, in accordance with theoretical predictions (Radhakrishnan and McConnell, 2000; Radhakrishnan *et al*, 2000), is probably a morphologic manifestation of an increased cholesterol activity. The importance of raft structures for epidermal biology, cholesterol metabolism, and lipid barrier formation may be fascinating areas of future studies.

The major finding of this study is evidence suggesting that lipid rafts are crucially involved in the regulation of oxidative stress in keratinocytes. First, both the baseline and UVA-induced synthesis of ROS tended to be higher in cells with well-developed raft structures (FITC-CTx^{high}). Second, ROS synthesis was dramatically reduced in cells in which rafts were disrupted with methyl-β-cyclodextrin, filipin, or exogenous ganglioside GM1. Third, ROS response was restored by replenishment of cholesterol in cells treated with methyl-β-cyclodextrin. The limitation of the methodology chosen for ROS assay (oxidation of the fluorescent probe carboxy-H_2DCFDA) does not allow us to determine which type of free radical is regulated via rafts. Our experience with this probe in HaCaT cells indicates that both at the baseline and after UVA irradiation carboxy-H_2DCFDA is mainly oxidized by H_2O_2 (Gniadecki *et al*, 2001). There is possibly a significant contribution from other types of radicals, however, such as NO derivatives or even singlet oxygen. There is a theoretical danger that carboxy-DCF production after UVA1 irradiation does not reflect endogenous ROS synthesis but rather a photochemical reaction in which the intracellularly trapped carboxy-2′,7′-dichlorodihydrofluorescein acts as a photosensitizer and is directly oxidized by UVA in the presence of oxygen. Data exist demonstrating that 2′,7′-dichlorofluorescein can be photoreduced by visible light into a semiquinone-type free radical, which may further be regeneratively oxidized by oxygen into superoxide (Marchesi *et al*, 1999). We consider this possibility unlikely in view of the fact that 2′,7′-dichlorodihydrofluorescein and 2′,7′-dichlorofluorescein absorb poorly in the UVA1 range (Molecular Probes Handbook, available on web site http://www.probes.com) and in view of the inability of UVA1 to induce appreciable carboxy-DCF fluorescence in both 2′,7′-dichlorodihydrofluorescein and carboxy-H_2DCFDA.

Although not directly addressed in this study, we briefly discuss the possible molecular mechanism by which rafts modulate intracellular ROS synthesis. The first issue to be resolved is whether the lipid component (e.g., higher chemical activity of cholesterol) or instead the raft- compartmentalized proteins are involved in the generation of ROS. The finding that exogenous GM1 ganglioside reduces ROS levels supports the latter notion. In contrast to methyl-β-cyclodextrin and filipin, which primarily target cholesterol, GM1 ganglioside causes a dissociation of proteins from rafts (Simons *et al*, 1999). Some signaling proteins (such as EGF and PDGF receptors, Ras, Rac, phosphatidylinositol 3-kinase) seem to be able to form complexes with membrane oxidases and thus induce H_2O_2 as a second messenger (Pennisi, 1997; Schlessinger, 2000). If such membrane-bound oxidase complexes exist, it is conceivable that they become active and produce ROS when segregated to rafts. ROS synthesized at plasma membranes may be involved in the amplification of oxidative stress, e.g., via the recently described positive feedback loop involving mitochondrial permeability transition pores (so-called mitochondrial ROS-induced ROS release) (Zorov *et al*, 2000; Gniadecki *et al*, 2001). Alternatively, changes in membrane fluidity by oxidative processes could alter the activity of oxidases, as shown recently for mitochondrial membranes (Ricchelli *et al*, 1999). Further progress in the understanding of the cellular regulation of oxidative stress may lead to novel therapeutic interventions relevant for photoprotection and cutaneous oncology.

The authors would like to thank Mrs Ingelise Pedersen and Mrs Vibeke Pless for technical help. Professor Barbara Gajkowska provided the GM1 ganglioside. The work of Dr. Jana Vicanova helped to generate the ideas important for this study. Financial support was obtained from Bang's Foundation, Haensch's Foundation, and Novo Nordisk Foundation.

REFERENCES

Bae GU, Seo DW, Kwon HK, et al: Hydrogen peroxide activates p70^{S6k} signaling pathway. *J Biol Chem* 274:32596–32602, 1999

Bae YS, Sung JY, Kim OS, Hur KC, Kazlauksas A, Rhee SG: Platelet-derived growth factor-induced H_2O_2 production requires activation of phosphatidylinositol 3-kinase. *J Biol Chem* 275:10527–10531, 2000

Boukamp P, Petrussevska RT, Breitkreutz D, Hornung J, Markham A, Fusenig N: Normal keratinisation in a spontaneously immortalized aneuploid human keratinocyte cell line. *J Cell Biol* 106:761–771, 1988

Chance B, Sies H, Boveris A: Hydroperoxide metabolism in mammalian organs. *Physiol Rev* 59:527–605, 1979

Chen Q, Ames BN: Senescence-like growth arrest induced by hydrogen peroxide in human diploid fibroblast F65 cells. *Proc Natl Acad Sci USA* 91:4130–4134, 1994

Clatch RJ, Foreman JR, Walloch JL: Simplified immunophenotypic analysis by laser scanning cytometry. *Cytometry* 34:3–16, 1998

Fagan KA, Smith KE, Cooper DMF: Regulation of the Ca^{2+}-inhibitable adenylyl cyclase type IV by capacitative Ca^{2+} entry requires localization in cholesterol-rich domains. *J Biol Chem* 275:26530–26537, 2000

Fra AM, Williamson E, Simons K, Parton RG: Detergent-insoluble glycolipid microdomains in lymphocytes in the absence of caveolae. *J Biol Chem* 269:30745–30748, 1994

Furuchi T, Anderson RGW: Cholesterol depletion of caveolae causes hyperactivation of extracellular signal-related kinase (ERK). *J Biol Chem* 273:21099–21104, 1998

Gniadecki R, Thorn T, Vicanova J, Petersen AB, Wulf HC: Role of mitochondria in ultraviolet-induced oxidative stress. *J Cell Biochem* 80:216–222, 2001

Hansford RG, Hogue BA, Mildaziene V: Dependence of H_2O_2 formation by rat heart mitochondria on substrate availability and donor age. *J Bioenerg Biomembr* 129:89–95, 1997

Harder T, Scheiffele P, Verkade P, Simons K: Lipid domain structure of the plasma membrane revealed by patching of membrane components. *J Cell Biol* 141:929–942, 1998

Hockberger PE, Skimina TA, Centonze VE, et al: Activation of flavin-containing oxidases underlies light-induced production of H_2O_2 in mammalian cells. *Proc Natl Acad Sci USA* 96:6255–6260, 1999

Irani K, Xia Y, Zweier JL, et al: Mitogenic signalling mediated by oxidants in Ras-transformed fibroblasts. *Science* 275:1649–1652, 1997

Janes PW, Ley SC, Magee AI: Aggregation of lipid rafts accompanies signaling via the T cell antigen receptor. *J Cell Biol* 147:447–461, 1999

Lu YP, Lou YR, Yen P, Newmark HL, Mirochnitchenko OI, Inouye M, Huang MT: Enhanced skin carcinogenesis in transgenic mice with high expression of glutathione peroxidase or both glutathione peroxidase and superoxide dismutase. *Cancer Res* 57:1468–1474, 1997

Mañes S, Mira E, Gómez-Moutón C, Lacalle RA, Keller P, Labrador JP, Martinez AC: Membrane raft microdomains mediate front-rear polarity in migrating cells. *EMBO J* 18:6211–6220, 1999

Marchesi E, Rota C, Fann YC, Chignell CF, Mason RP: Photoreduction of the fluorescent dye 2′-7′-dichlorofluorescein: a spin trapping and direct electron spin resonance study with implications for oxidative stress measurements. *Free Radic Biol Med* 26:148–161, 1999

Melkonian KA, Ostermeyer AG, Chen JZ, Roth MG, Brown DA: Role of lipid modifications in targeting proteins to detergent-resistant membrane rafts. Many raft proteins are acylated while few are prenylated. *J Biol Chem* 274:3910–3917, 1999

Moran M, Miceli M: Engagement of GPI-linked CD48 contributes to TCR signals and cytoskeletal reorganization: a role of lipid rafts in T cell activation. *Immunity* 9:787–796, 1998

Morita A, Werfel T, Stege H, *et al*: Evidence that singlet oxygen-induced human T helper cell apoptosis is the basic mechanism of ultraviolet-A radiation phototherapy. *J Exp Med* 186:1763–1738, 1997

Nohl H, Jordan W: The mitochondrial site of superoxide formation. *Biochem Biophys Res Commun* 138:533–539, 1986

Osborn M, Johnsson N, Wehland J, Weber K: The submembranous location of p11 and its interaction with the p36 substrate of pp60 src kinase *in situ*. *Exp Cell Res* 175:81–96, 1988

Pennisi E: Superoxides relay Ras protein's oncogenic message. *Science* 275:1567–1568, 1997

Quillet-Mary A, Jaffrezou JP, Mansat V, Bordier C, Naval J, Laurent G: Implication of mitochondrial hydrogen peroxide generation in ceramide-induced apoptosis. *J Biol Chem* 272:21388–21395, 1997

Radhakrishnan A, Anderson TG, McConnell HM: Condensed complexes, rafts, and the chemical activity of cholesterol in membranes. *Proc Natl Acad Sci USA* 97:12422–12427, 2000

Radhakrishnan A, McConnell HM: *Biochemistry* 39:8119–8124, 2000

Ricchelli F, Gobbo S, Moreno G, Salet C: Changes of the fluidity of mitochondrial

membranes induced by the permeability transition. *Biochemistry* 38:9295–9300, 1999

Roy S, Luetterforst R, Harding A, et al: Dominant-negative caveolin inhibits H-Ras function by disrupting cholesterol-rich plasma membrane domains. *Nature Cell Biol* 1:98–105, 1999

Sankaram MB, Thompson TE: Interaction of cholesterol with various glycerophospholipids and sphingomyelin. *Biochemistry* 29:10670–10675, 1990

Scheiffele P, Roth MG, Simons K: Interaction of influenza virus haemagglutinin with sphingolipid-cholesterol membrane domains via its transmembrane domain. *EMBO J* 16:5501–5508, 1997

Schlessinger J: Cell signaling by receptor tyrosine kinases. *Cell* 103:211–225, 2000

Simons K, Ikonen E: Functional rafts in cell membranes. *Nature* 387:569–572, 1997

Simons K, Toomre D: Lipid rafts and signal transduction. *Nature Rev Mol Cell Biol* 1:31–38, 2000

Simons M, *et al:* 1999. Exogenous administration of gangliosides displaces GPI-anchored proteins from lipid microdomains in living cells. *Mol Biol Cell* 10:3187–3196, 1999

Stauffer TP, Meyer T: Compartmentalized IgE receptor-mediated signal transduction in living cells. *J Cell Biol* 139:1447–1454, 1997

Wilson BS, Pfeiffer JR, Oliver JM: Observing FcεRI signaling from the inside of the mast cell membrane. *J Cell Biol* 149:1131–1142, 2000

Xavier R, Brennan T, Li Q, McCormack C, Seed B: Membrane compartmentation is required for efficient T cell activation. *Immunity* 8:7123–7732, 1998

Zamzami N, Marchetti P, Castedo M, *et al*: Sequential reduction of mitochondrial transmembrane potential and generation of reactive oxygen species in early programmed cell death. *J Exp Med* 182:367–377, 1995

Zorov DB, Filburn CR, Klotz LO, Zweier JL, Sollott SJ: Reactive oxygen species (ROS)-induced ROS release: a new phenomenon accompanying induction of the mitochondrial permeability transition in cardiac myocytes. *J Exp Med* 192:1001–1014, 2000